

Transport gap in a $\nu = 1/3$ quantum Hall system : a probe for skyrmions

Annelene F. Dethlefsen and Rolf J. Haug

Institut für Festkörperphysik, Universität Hannover, Appelstraße 2, D-30167 Hannover, Germany

Karel Vybomý and Ondřej Čertík

Fyzikální ústav, Akademie věd České republiky, Cukrovarnická 10, CZ-16253 Praha 6, Czech Republic and
1. Institut für theoretische Physik, Universität Hamburg, Jungiusstr. 9, D-22305 Hamburg, Germany

Arkadiusz Wojs

Institute of Physics, Wrocław University of Technology,
Wybrzeże Wyspiańskiego 27, 50-370 Wrocław, Poland
(Dated: March 17th, 2006)

The dependence of the activated gap on magnetic field is studied for the fractional filling factor $1/3$. By comparing the experimental results with results from exact diagonalization calculations we are able to identify the excitation of a small antiskyrmion in the low-field regime and a cross-over to spinless excitations at higher magnetic fields. The effect of sample quality is studied. On the side of the theory, comparison between different geometries (torus and sphere) and different sizes is carried out. Under inclusion of Landau level mixing and finite thickness, we obtain a good agreement between calculated energies and experimental results.

PACS numbers: 73.43.-f, 73.43.Lp, 75.10.Jm, 72.10.Fk, 73.63.-b

I. INTRODUCTION

The existence of skyrmions is one of the remarkable many-body phenomena accompanying the quantum Hall effects. After the skyrmions were established^{1,2,3,4} in the integer quantum Hall effect (IQHE) a question appeared whether they can also be observed in the regime of the fractional quantum Hall effect (FQHE), given the composite fermion (CF) mapping between the IQHE and the FQHE⁶. We report here on an experiment indicating that the answer is positive.

A skyrmion can be viewed as a finite-size quasiparticle of charge e located at r_0 in the parent ground state, which is e.g. the fully polarized (\uparrow) completely filled lowest Landau level (LL). More precisely, it is the many-body ground state at magnetic field B corresponding to the filling factor $\nu = (n_e h/eB) = 1$ minus one magnetic flux quantum (n_e is the electronic density, h Planck's constant and e the elementary charge of an electron). In this state, called also a spin-texture, the expectation value of spin is reversed (\downarrow) at $r = r_0$, it remains unchanged (\uparrow) for $r \neq r_0$ and it interpolates smoothly between r_0 and infinity⁷. A size, K (precise definition in Sec. III), can be attributed to a skyrmion, related to how fast the spin changes with displacement from the skyrmion center. For magnetic fields of $\nu = 1$ plus one magnetic flux quantum a symmetric quasiparticle of charge $-e$ exists, an antiskyrmion.

The skyrmions at integer filling factors can either be studied using Hartree-Fock⁷ and field theoretic methods^{8,9,10} on one side or by exact diagonalization^{11,12,13} on the other side and all these approaches are interrelated¹⁴. The central conclusion is that while Zeeman energy prefers small sizes K , meaning small average number of reversed spins,

the Coulomb (exchange) energy prefers spatially smooth spin textures, i.e. large skyrmions, where two neighbouring spins are almost parallel. The size of the skyrmion lowest in energy is thus determined by the ratio of the Zeeman and Coulomb energies, $\nu_0 = E_Z/E_C = \mu_B g B / (e^2 / (4\pi\epsilon_0)) / \mu_B$, where $\mu_0 = \hbar/eB$ is the magnetic length, μ_B the Bohr magneton, g the effective electronic Landé factor and ϵ_0 the dielectric constant. This conclusion remains valid also for integer filling factors¹⁵ $\nu > 1$, albeit the nonmonotonous Haldane pseudopotentials imply richer skyrmion phase diagram¹².

Works related to fractional filling factors^{8,12,16,17}, most importantly to $\nu = 1/3$ which is the CF counterpart to $\nu = 1$ of electrons, lead to the same conclusion. However, apart of quantitative differences in skyrmion energies, fractional and integer systems showed some qualitative differences. The exact symmetry between skyrmions ($\nu > 1/3$) and antiskyrmions ($\nu < 1/3$) is absent¹² and thus skyrmion and antiskyrmion sizes need not be the same in one system. Also, temperature dependences of the magnetization are different in the IQHE and FQHE regimes^{18,19}.

Experimentally, the skyrmions were proven in magnetotransport and in the Knight shift of the NMR or magnetooptical spectroscopy sensitive to the spin polarization of the 2DEG. The first method probes skyrmion (antiskyrmion) pairs as an excitation on the background of the fully spin polarized (ferromagnetic) ground state at exactly $\nu = 1$. The other two methods probe the ground state at a slightly changed filling factor. Provided the filling factor is not too far from one, the ground state remains the ferromagnetic state plus one skyrmion (antiskyrmion) per magnetic flux removed (added) to the system. The depolarization in units of electron spin per

one magnetic flux is thus equal to the average size of a skyrmion, i.e. to the number of involved spin flips.

From the transport activation gap at filling factor one, Schmeier et al.² concluded that a typical excitation in a GaAs heterostructure contains seven spin flips. If the excitation is a skyrmion (antiskyrmion pair, each of these should have a size of $K = 3$). The number of spin flips (size) was found to decrease with increasing ratio of Zeeman and Coulomb energies. The optical experiments³ and the NMR experiments¹ gave approximately the same result. Hydrostatic pressure reduces the effective Lande g -factor in GaAs and even $g = 0$ is experimentally possible. It allows to access smaller values of ν compared to performing measurements at low magnetic fields where QHE will eventually disappear. Maude et al.⁴ observed skyrmions as large as $K = 16$ in magnetotransport at nearly vanishing Zeeman energy.

The Coulomb energy stabilizing skyrmions is much smaller at $\nu = \frac{1}{3}$ as compared to $\nu = 1$. As a consequence, the skyrmions in the FQHE regime are usually smaller. Leadley et al.⁵ found excitations with three spin flips in magnetotransport at nearly $g = 0$ implying skyrmion sizes (K_S) and antiskyrmion sizes (K_A) with $K_A + K_S + 1 = 3$. In contrast to this, NMR measurements by Khandelwal et al.²⁰ suggested $K_A = K_S = 0.1$. The reason for this very different result is unclear.

Experimental arguments in favour of skyrmions at $\nu = \frac{1}{3}$ are by far not so numerous as compared to integer filling factors. With our new experiments agreeing well with exact diagonalization calculations presented here, we believe, the existence of skyrmions in the FQHE is confirmed as well as the skyrmion-antiskyrmion asymmetry demonstrating the qualitative differences between electrons and composite fermions.

To demonstrate the influence of the sample quality we present measurements of the $\nu = \frac{1}{3}$ activation gap, E_a , from two gated heterostructures as a function of the electron density n_e , i.e. the magnetic field B , Sec. II. We observe a linear (B) behaviour in a large region of magnetic fields implying that, roughly, the probed excitation costs much Zeeman energy and little Coulomb energy. In particular, the lowest excitation in the high mobility sample contains two spin flips while it has a single spin flip for the low mobility sample. While the latter case corresponds to a spin wave, a quasihole (QH) and a quasielectron with reversed spin (QEr), the excitation with two spin flips must contain either a skyrmion or an antiskyrmion. Energies obtained by exact diagonalization (ED) support this interpretation, Subsec. IIIC, and they indicate that we observe a pair of the QEr and the smallest antiskyrmion, the one containing one spin flip.

Moreover we observe a clear transition to another lowest excited state for $B \approx 9$ T in the high mobility sample. The energies obtained by the ED suggest that the relevant excitation then contains no spin flip. This agrees with the usual statement that such excitations in the high B limit are the charge density waves (CDW) with very large wavevector k . However, in the present case

we observe a remarkable coincidence between the activation gap and the magnetoroton minimum, i.e. CDW at $k_0 \approx 1.4$. We propose that this could be because the activation is a two-step process where creation of a magnetoroton is a bottleneck.

The exact diagonalization calculations, Sect. III, start with ideal systems (zero width, ~ 1 μm , $e^2 = (4\pi\epsilon_0\epsilon_r)^{-1}$) and then we take into account the finite thickness of the 2D electron gas as well as the LL mixing. Assuming a B field independent reduction^{21,22} E_d of the activation gaps due to the disorder ubiquitous in experimental samples, the calculated energies lead to a quantitatively correct prediction of the activation gap with a single fitting parameter E_d .

II. THE EXPERIMENT

The investigated two-dimensional electron systems are realized in $\text{Al}_{0.33}\text{Ga}_{0.67}\text{As/GaAs}$ heterostructures. The sample growth parameters are given in Tab. I. The basic

sample	spacer-width	density (m^{-2})	mobility (m^2/Vs)
		$T = 40$ mK, dark	$T = 40$ mK, dark
# 1	70 nm	$1.3 \cdot 10^{15}$	700
# 2	40 nm	$1.6 \cdot 10^{15}$	79

TABLE I: Parameters of the investigated samples.

difference between the samples is their mobility. The high quality of sample # 1 allows to study several different FQHE states, whereas the mobility below $100 \text{ m}^2/\text{Vs}$ is sufficient only for studies of the most robust FQHE state, $\nu = 1/3$, in sample # 2.

A metallic topgate enables us to vary the electron density in a wide range. For sample # 1 the electron density n_e is varied between 0.2 and $1.3 \cdot 10^{15} \text{ m}^{-2}$ with a zero field mobility reaching $700 \text{ m}^2/\text{Vs}$ at 40 mK. With sample # 2, densities between 0.59 and $1.6 \cdot 10^{15} \text{ m}^{-2}$ can be accessed. Here the zero field mobility reaches $79 \text{ m}^2/\text{Vs}$ at 40 mK.

The experiments are performed in a dilution refrigerator with magnetic fields up to 20 T. The longitudinal resistivities ρ_{xx} (Shubnikov de Haas oscillations) of the two samples at nearly the same electron densities are shown in Fig. 1 demonstrating the different quality of the samples. While the sample # 2 exhibits only one minimum between filling-factors $\nu = 1$ and $\nu = 1/3$, for sample # 1 there is a series of different fractional quantum Hall states in this region.

To obtain the activation energy for the different magnetic fields we investigate the temperature dependence of the resistivity minimum at $\nu = 1/3$. The temperatures in our experiment are varied between $T = 40$ mK and 1000 mK. In this range the error of measurement of the calibrated ruthenium oxide sensor is 1 mK. We extract the gap out of Arrhenius plot data, using the

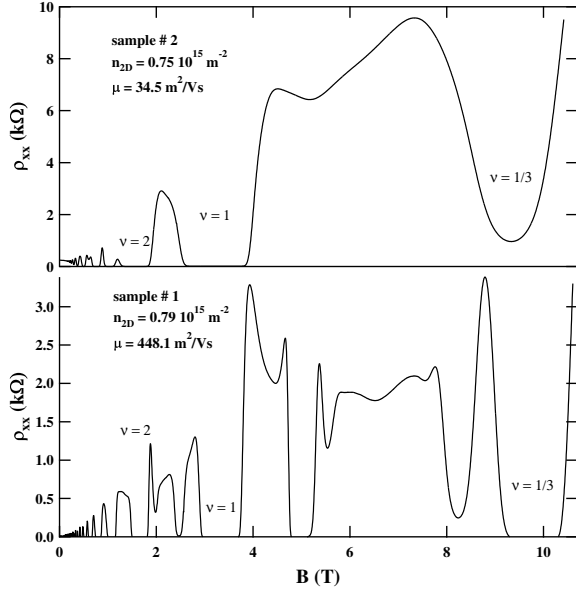


FIG. 1: Shubnikov-de Haas oscillations for both samples at similar electronic densities.

activated resistance behaviour $\rho_{xx} \propto \exp(-\Delta/2T)$. We assume that our total uncertainty in Δ is less than 2%. The measured activation energies are shown in Fig. 2 for the two samples.

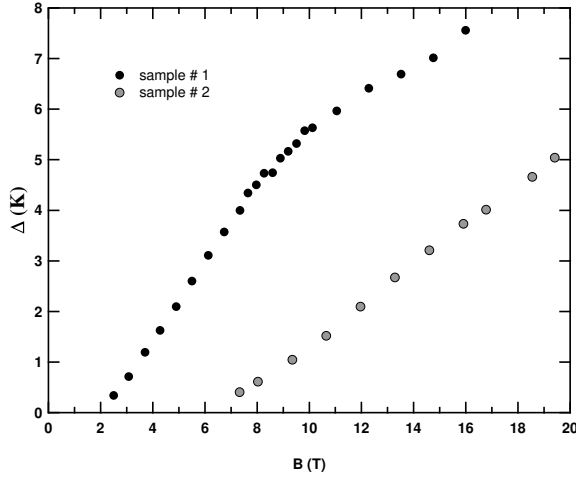


FIG. 2: Gap energies at $\nu = 1/3$ from sample #1 and #2.

III. EXACT DIAGONALIZATION

Electron-electron interaction is the fundamental effect giving rise to most of the phenomena occurring within the lowest LL. Because of the extremely high degeneracy of LLs, standard techniques like Hartree-Fock approxi-

mation are inapplicable for describing these phenomena.

In the exact diagonalization (ED) approach^{25,26}, we start with the complete many-body Hamiltonian. It comprises of the electron-electron interaction and the Zeeman energy.

$$H = \sum_{\mathbf{j}} \sum_{\mathbf{j}'} A_{\mathbf{j}\mathbf{j}'} c_{\mathbf{j}_1}^y c_{\mathbf{j}_2}^y c_{\mathbf{j}_3}^y c_{\mathbf{j}_4}^y + \sum_{\mathbf{j}} E_Z \frac{1}{2} c_{\mathbf{j}}^y c_{\mathbf{j}}^y \quad (1)$$

$$\mathbf{j} = (j_1; j_2; j_3; j_4); \quad \mathbf{j}' = (j'_1; j'_2)$$

Here j_i is the orbital quantum number, $s = \pm 1$ is the spin and c_j^y are the operators creating the corresponding one-electron states. A convenient one-particle orbital quantum number is either angular momentum or one component of the linear momentum. These choices are typical for spherical geometry and torus geometry, respectively. The last two notions describe the central approximation of the ED model. Instead of an infinite plane, we study a compact manifold preferably without edges, that is, we confine the electrons either to the surface of a sphere²⁷ or to a rectangle with periodic boundary conditions²⁸ (torus). The Coulomb matrix elements $A_{\mathbf{j}\mathbf{j}'}$ are given explicitly in Reference 29 for torus and they straightforwardly follow from the Haldane pseudopotentials on a sphere²⁷. The Zeeman energy is just $E_Z = \mu_B g B$.

For the moment, we did not include any cyclotron energy ($\sim \hbar \omega_c = \hbar e B / m$) term into (1). All electrons are assumed to stay in the lowest LL which is true for the ground state and low-lying excited states if $\hbar \omega_c \ll A_{\mathbf{j}\mathbf{j}'}; E_Z$ and $\hbar \omega_c \ll 2T$. This approximation, exclusion of the LL mixing, is justified in the high B limit owing to $\hbar \omega_c \ll E_Z \propto B$, $A_{\mathbf{j}\mathbf{j}'} \propto 1/B$ and $\hbar \omega_c \propto B$.

The homogeneous magnetic field in the 2D system now corresponds to $N_m = 2Q$ quanta of magnetic flux passing through the surface of the sphere or torus. In this situation, exactly N_m one-electron states exist in the system^{25,30}. If we now put N_e electrons into the system, the filling factor is $\nu = N_e / N_m$ for the torus and $\nu = N_e / (N_m + 1)$ for the sphere. The quantity ν is of the order of unity ($\nu \approx N_m \gg 0$ for $N_m \gg 1$) and it is related to the topology of the considered eigenstate³¹.

The number of all possible N_e -electron states is then finite. The matrix of Eq. (1) in this complete basis is evaluated and diagonalized yielding the energies and many-body wavefunctions.

A. Activation energy in transport

It has been widely accepted that the activation gap is the lowest energy needed to create a neutral pair of charged particles and to separate them very far from each other^{32,33}. Starting from the Laughlin ground state at $\nu = 1/3$, these particles are not an electron and a hole. Rather they are particle-like many-body excitations³⁴ with charge q and spin s . They are usually called quasi-electrons (QE, $q = 1/3, s = 1/2$) and quasiholes (QH, $q = -1/3, s = 1/2$), eventually with reversed spin (QEr,

$q = \frac{1}{3}, s = 1/2$) as regarding to the direction preferred by the Zeeman energy. Creation energies of all these three quasiparticles are different, even disregarding the Zeeman contribution, owing to their actual many-body nature. This is a fundamental difference to IQH systems.

Because of their charge $e=3$, all interactions between the mentioned quasiparticles at $\nu = 1/3$ (e.g. skyrmion energies discussed below) are roughly weaker by an order of magnitude compared to $\nu = 1$. The interactions at long range are similar to the common Coulomb repulsion or attraction because the size of the quasiparticles is of the order of λ_0 . At short range, on the other hand, it's not guaranteed that the interactions are similar to electrons because of the internal structure of the quasiparticles^{23,24}. Contrary to QE, the charge densities of QEr and QH are, however, basically structureless and this fact lies at the heart of the close analogy between low-energy excitations at $\nu = 1/3$ and $\nu = 1$.

The Coulomb energy of skyrmions and antiskyrmions can be obtained from the ED spectra on a sphere³⁵ in a system more, respectively, than what would correspond to $\nu = \frac{1}{3}$, Fig. 3. For $E_Z = A_J$, the lowest excitation to determine the activated transport will involve creation of a QE+QH pair. As E_Z decreases, the lowest excitation becomes QEr+QH, because the energy of a QEr (Coulomb 'correlation' energy) is lower¹² than the energy of a QE, Fig. 3 left. This will however not remain true in the limit $E_Z \rightarrow 0$. There are objects with even lower Coulomb energy than QEr and QH. For each $K = 1; 2; \dots$ there is one such object with total spin $K + 1/2$ and charge $e=3$ and $e=3$. They are usually called skyrmions (Sky) and antiskyrmions (ASky), respectively. Contrary to IQH systems, energies of Sky(K) and ASky(K) are different implying that the skyrmion size K_S and the antiskyrmion size K_A need not be equal in the same system. Sky(K) [ASky(K)] is the energy difference between the QEr [QH] and the lowest state with angular momentum and spin

$$L = L_{QEr/QH} - K; \quad S = S_{QEr/QH} - K; \quad (2)$$

In a system of N_e electrons, the angular momenta used are $L_{QH} = S_{QH} = N_e/2$ and $L_{QEr} = S_{QEr} = N_e/2 - 1$. With this definition, ASky(0) is a QH and Sky(0) is a QEr, meaning that ASky(K) contains K flipped spins while Sky(K) contains $K + 1$ flipped spins.

Figure 4 shows the competition between skyrmions of different sizes as a function of magnetic field, which means that the ratio between the Coulomb and Zeeman energies, β , is varied. The Zeeman energy prefers small skyrmions since these include less spins. Thus, for fields above 4.5 T (1.5 T) no antiskyrmions (skyrmions) occur in an ideal system as the Zeeman energy β/B is then too large compared to the binding (Coulomb) energy β/B . Owing to a rather high Coulomb energy cost, the QE becomes favorable over QEr first at rather high magnetic fields, Fig. 4 (left).

Once a neutral pair of quasiparticles, Sky(K_S) and

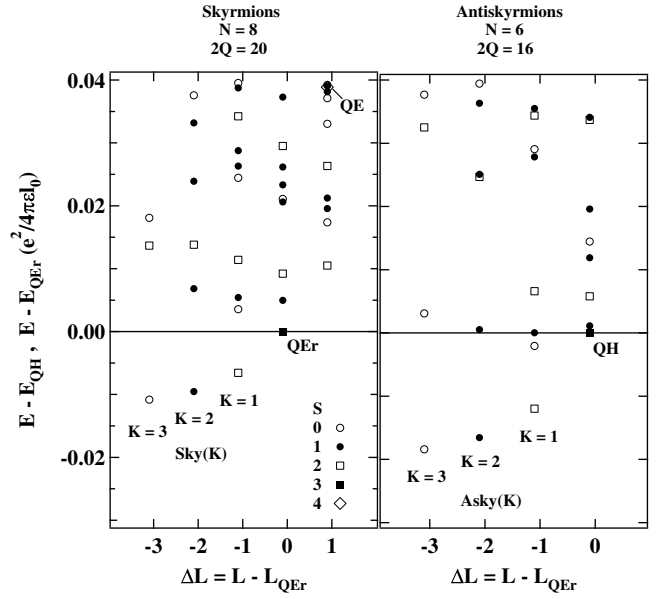


FIG. 3: Full skyrmion and antiskyrmion spectra at $\nu = \frac{1}{3}$ minus and plus one magnetic flux quantum respectively and zero Zeeman energy. The (anti)skyrmion branches of $L = K$ have negative energy and they are well separated from the continuum of excited states. For $\nu > \frac{1}{3}$, quasielectron with reversed spin (QEr) is lower in energy than QE. This holds for systems of all accessible sizes (here 6 and 8 electrons).

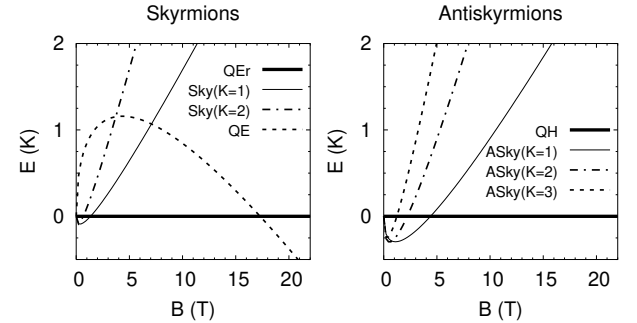


FIG. 4: Skyrmion and antiskyrmion energies at $\nu = \frac{1}{3}$ relative to QEr and QH in an ideal system with six electrons. The QE energy shown refers to the extrapolated $1/N \rightarrow 0$ values with finite thickness taken into account ($\beta = 0.3$).

ASky(K_A), has been created, they behave similarly to a magnetoexciton. In a magnetic field, the magnetoexciton has a constant linear momentum k which is proportional to the mutual distance x between the quasiparticles. In the classical approach we would expect its energy to be $E(x) \propto 1/x$ with proportionality constant determined by the charges of the two constituent quasiparticles. In the ED spectra such modes can be identified, Fig. 5. They are usually called magnetoroton (MR) branch, $E_{CDW}(k)$, for QE+QH and spin wave (SW), $E_{SW}(k)$, for QEr+QH. The limiting values for

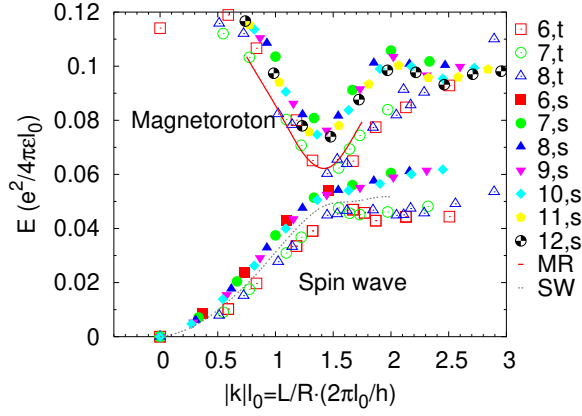


FIG. 5: The spin wave (SW) and the magnetoroton branch (MR) seen in the ED spectra of ideal $\nu = \frac{1}{3}$ systems of different sizes and geometries. In the legend, 't' stands for torus, 's' for sphere and the number indicates the number of electrons. The lines (solid and dotted) were obtained from the $1/N \rightarrow 0$ extrapolation of the data (MR and SW) on the sphere.

$k \neq 1$ are the energies necessary to create a QE + QH (QEr + QH) pair and to separate them far from each other. These are the quantities commonly used for comparison to the transport activation gaps, because the SW (MR) is the lowest excitation (at $k \approx 1.0 \cdot 10^{-1}$) among all states with total spin $S = N - 2 \cdot 1$ ($S = N - 2$), i.e. with one (with no) spin flip.

It is remarkable how much $E_{CDW}(k)$ calculated on a sphere and on a torus differ, on a quantitative level, Fig. 5. Even though the positions of the magnetoroton minimum match well in both geometries ($k_0 \approx 1.4$), sphere gives seemingly a higher energy of the minimum by as much as 20%. A careful extrapolation to infinite systems (solid line in Fig. 5) however matches excellently the results obtained on a torus. This is not surprising, given the magnetoexcitonic character of the MR. The MR of a comparable to the radius of the sphere will have the QE and the QH located near the opposite poles. Such situation is not compatible with a picture of a plane wave of $k = x = \frac{2}{l_0}$ propagating along the equator. On the other hand, with increasing radius of the sphere R this becomes a finite size effect if $R \propto x$. Based on Fig. 5, we believe finite system data from the torus are more suitable to give quantitative estimates for magnetoroton and spin wave energies.

For a Sky (K_S) - ASky (K_A) pair, we take $E_{SW}(k)$ with $k \neq 1$ and add the creation energies of Sky (K_S) and of ASky (K_A). Instead of one system, as it was the case for studying the QEr + QH pair, we thus have to exactly diagonalize three different systems: one for the quasiparticle-separation procedure, one for the Sky and one for the ASky. This more complicated procedure suffers possibly less from the finite size effects, since skyrmions are rather extended objects, in particular more extended than a bare QH or QEr. Recall that sizes of Sky and ASky

need not be the same.

B. Finite thickness and LL mixing

Adding to the description of experiments under realistic conditions, three ever valid facts should not be left unnoticed: the sample is actually three-dimensional (finite extent of the wavefunction perpendicular to the 2DEG), the magnetic field is finite (mixing between Landau levels) and the system is never perfectly homogeneous (disorder).

Non-zero thickness w of the 2DEG can be effectively incorporated into the Haldane pseudopotentials²⁷ which completely determine the Hamiltonian of the lowest LL. Qualitatively, the larger the effective thickness $w = l_0$, the more softened becomes the effective electron-electron interaction on shortest distances.

Quantitative effects of the presence of the third dimension have been studied since the early times of the FQHE, both with the Laughlin state³⁶ and the activation gap³⁷. In a heterostructure, electrons are confined to a nearly triangular potential well. A standard choice for the wavefunction in the growth direction is then the Fang-Howard trial wavefunction³⁸, $\Psi_{FH}(z) = (b^3/2)^{1/2} z e^{bz/2}$. We will mostly stay with this choice, even though we are aware of other options for $\Psi(z)$ which may lead to slightly lower subband energies (Sec. V in Morf et al.³⁹). Differences originating from these different choices of $\Psi(z)$ should be smaller than the uncertainty in the variational parameter b (or the thickness of the 2DEG) relevant for our experiments. This has been checked with $\Psi_{QW}(z) = \cos az$, $|z| < \pi/2$, relevant for symmetric quantum wells. Taking $\Psi_{FH}(z)$ instead of $\Psi(z)$ is equivalent³⁷ to using a nontrivial form for $F(q)$ in the 2D Fourier transform $S_V(q)$ of the Coulomb interaction

$$V(q) = \frac{F(q)}{q}; \quad F(q) = \frac{8 + 9(q=b) + 3(q=b)^2}{(2 + 2q=b)^3}; \quad (3)$$

The quantity $V(q)$ then enters the Coulomb matrix elements in (1) as given in standard references^{25,40}. These can be in turn reexpressed in terms of the Haldane pseudopotentials⁴¹ V_m . For reasonable values of b , only V_0 changes appreciably, it decreases by 25% for $b^{-1} = 0.3 l_0$.

Spatial extent of the wavefunction along z defined as FWHM is $w = 4/9 = b$ for Ψ_{FH} and $w = \frac{2}{3} = a$ for Ψ_{QW} . The wavefunction parameter b depends on the form (steepness) of the triangular well potential and therefore it is not constant but it changes with the applied gate voltage. This leads to^{37,38}

$$b = [33 m e^2 n_e / 2 \pi^2]^{1/3}; \quad (4)$$

which depends only on the electron density²⁵ n_e and the dielectric constant ϵ . If we assume the filling factor fixed to $1/3$, the density becomes a function of the magnetic

eld, so that

$$= (b_0)^{-1} \approx 0.23 \quad (B [T])^{-6} : \quad (5)$$

This is a formula relevant for both our samples.

The LL mixing is more difficult to include. If we admit that higher Landau levels may also be populated even at $\beta < 1$, we must (i) add the cyclotron energy term $\epsilon_{n,j} = (n+1/2)\hbar\omega_c$ to the Hamiltonian (1). We also have to considerably extend the many-body basis (ii) because we have introduced a new single-particle orbital quantum number, the Landau level index n . The former fact also implies that we have a new energy scale $\hbar\omega_c/B$ in the problem. Recall here the criterion for the neglect of LL mixing: $1/\omega_c \ll \tau$. Fortunately, the magnetic fields relevant for the FQHE are still high enough for LL mixing to be treated perturbatively. In practice this means, that in the first (second) order we allow for maximum one (two) particles to be in the first LL ($n=1$) when constructing the many-body basis. For the current purpose we allowed for up to two particles in the first Landau level and verified in small systems that increasing this number does not change the energies perceptibly.

Without higher LLs, the energies E_C of Hamiltonian's (1) Coulomb part were conveniently evaluated in the Coulomb units $e^2/(4\pi\epsilon_0)$. Then the energies were magnetic-field-independent for $E_Z = 0$ and depended via S_z trivially on B for $E_Z \neq 0$, in particular $E_Z = (e^2/(4\pi\epsilon_0))/S_z B$. With other LLs included in addition to the lowest one, $E_C = (e^2/(4\pi\epsilon_0))$ becomes a function of B or better of $\beta = \hbar\omega_c/(k_B T) = (e^2/(4\pi\epsilon_0))/k_B T$. However, since variations of $E_C = (e^2/(4\pi\epsilon_0))$ as a function of B (β) are typically small, see Fig. 6, we will adhere to the Coulomb units.

Disorder is to the best of our knowledge the only relevant effect not described microscopically within this work. A common notion is that the disorder reduces the incompressibility gap⁴². In fact, randomly distributed potential impurities included into the system (1) change energies of both the ground state and the excited state. Because the excited states in question consist of two microscopic quasiparticles on the background of the Laughlin ground state, we will assume for our purposes that the disorder indeed reduces the excitation energy by a constant^{21,22}. The reduction E_d is typically of the order of one Kelvin. It need not be the same for different excitations (skyrmions, magnetorotons) and this causes probably the largest uncertainty in the respective energies of spin textures of different sizes. Values of magnetic field where transitions occur remain the same as in the disorder-free systems, Fig. 4, only as long as the gap reduction is equal for the two involved excitations.

C. Numerical data

Finite thickness of the 2DEG and LL mixing do not change the SW and MR dispersions qualitatively. Their

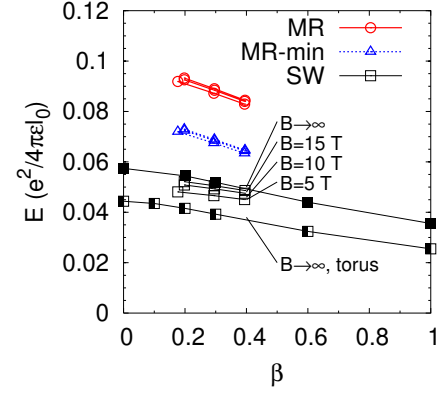


FIG. 6: The effect of the finite thickness and the LL mixing on the magnetoroton (MR) minimum and on the best approximation to the $k \rightarrow 1$ energies of the spin wave (SW) and the MR branch. Finite system (seven electrons) on a sphere is considered, except the single curve marked 'torus'. Energies labeled with B include the Landau level mixing which vanishes for $B \rightarrow \infty$.

effect is that the ideal dispersions $E_{CDW}(k)$ and $E_{SW}(k)$ become multiplied by a nearly k -independent coefficient. The limiting values for $k \rightarrow 1$ are reduced, both for nonzero thickness and LL mixing, Fig. 6. For experimentally relevant values of the parameters, finite thickness decreases $E_{SW}(k \rightarrow 1)$ by 10% (for $\beta = 0.3$) and the LL mixing up to the second order decreases $E_{SW}(k \rightarrow 1)$ by 10% (at $B = 5$ T).

Our best estimate for $E_{SW}(k \rightarrow 1)$ starts with the torus. It includes finite thickness ($\beta = 0.3$) and LL mixing (as of $B = 5$ T) and it reads $0.035e^2/(4\pi\epsilon_0)$. Fig. 5 suggests that this value almost would not change if we studied larger systems. Note that with increasing magnetic field of the heterojunction increases, Eq. (5), while the LL mixing becomes less important. Quantitatively, the latter effect is stronger so that the indicated value of $E_{SW}(k \rightarrow 1)$ in Coulomb units will slightly increase with increasing magnetic field, cf. Fig. 6.

	torus		sphere			
	ideal	finite width $\beta = 0.3$	ideal	finite width $\beta = 0.3$	+ LL mixing $B = 5$ T	+ tdyn limit $1/N \rightarrow 0$
SW	0.045	0.039	0.057	0.052	0.047	
MR	0.093	0.080	0.102	0.089	0.087	
MR-min	0.063	0.054	0.076	0.069	0.067	
Sky (1)			-0.0062	-0.0056	-0.0065	-0.0050
ASky (1)			-0.0112	-0.0102	-0.0118	-0.0088
QE			0.0385	0.0335	0.0424	0.0222

TABLE II: Energies in $e^2/(4\pi\epsilon_0)$ concerning Fig. 6 (SW, MR, MR-min) and Fig. 7 (Sky (1), ASky (1), QE).

The skyrmion and antiskyrmion spectra at $\beta = \frac{1}{3}$ have been introduced in the previous paragraph, Fig. 3. At the magnetic fields of our experiment only the smallest

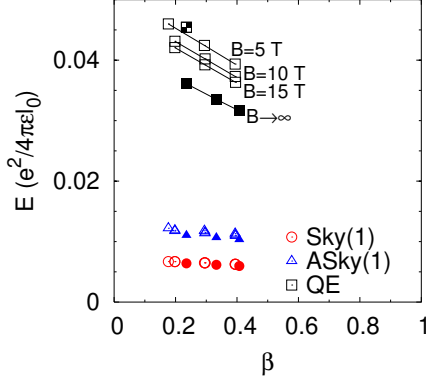


FIG. 7: Analogous to Fig. 6 but for the QE energy relative to the energy of QEr as well as for energies of the smallest skyrmion and antiskyrmion. All data were obtained on a sphere, solid symbols refer to energies under no LL mixing.

(anti)skyrmions are possible, Fig. 4. Contrary to the spin wave: Their condensation energies relative to a bare QEr and QH, show a slight dependence on the system size, Fig. 8. A linear fit in $1/N$ leads to (anti)skyrmion energies by about 10% lower at $1/N \rightarrow 0$ than they are for $N_e = 7$, Fig. 7 and Table II. In contrast to this, the QE energy becomes reduced by as much as 35%.

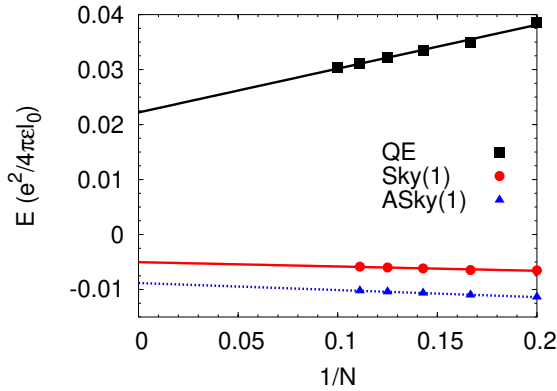


FIG. 8: Extrapolation of the (anti)skyrmion and QE energies to the thermodynamical limit $1/N_e \rightarrow 0$. Sphere, no LL mixing, $\ell = 0.33$.

The finite thickness ($\ell = 0.3$) also reduces the Sky(1), ASky(1) and QE energies by about 10%, 10% and 20%, respectively. On the other hand, the Landau level mixing (1st order, $B = 5$ T) increases these energies by 20%, 15% and 25%, respectively, Fig. 7 and Table II. The best guesses for the energies in $e^2/(4\pi\ell_0)$ relevant to our experiment is the following: 0.0058 for Sky(1) and 0.0102 for ASky(1) for $B = 5$ T and a thickness corresponding to $\ell = 0.3$ and 0.0240 for QE at $B = 15$ T and $\ell = 0.4$. All these energies will definitely be reduced when magnetic field is swept up because both LL mixing

and finite thickness have this tendency.

The data extracted from Fig. 6 and 7 are summarized in Table II.

IV. INTERPRETATION OF THE EXPERIMENTAL DATA

The B dependence of the activation gap in the sample # 1 shows an apparent transition slightly below 10 T. Let us divide the investigated range of magnetic field into three regions as shown in Fig. 9: I (low field), II (transition) and III (high field).

In the following we wish to argue that the lowest excitation which determines the activation gap in region I is a QEr{antiskyrmion ($K_A = 1$)} pair. In region III, QE{QH} pairs without spin flip are observed while the QEr{QH} pairs likely show up in region II.

Our discussion begins with a general observation that the gap can change either / B (Zeeman energy) or / \sqrt{B} (Coulomb energy)

$$[K] = E_C \sqrt{50.2 B [\text{T}]} + (S_z \sim) 0.295 B [\text{T}] \quad (6)$$

Here the Coulomb energy E_C should be put in units $e^2/(4\pi\ell_0)$ and $(S_z \sim)$ means the number of spins flipped in the excitation.

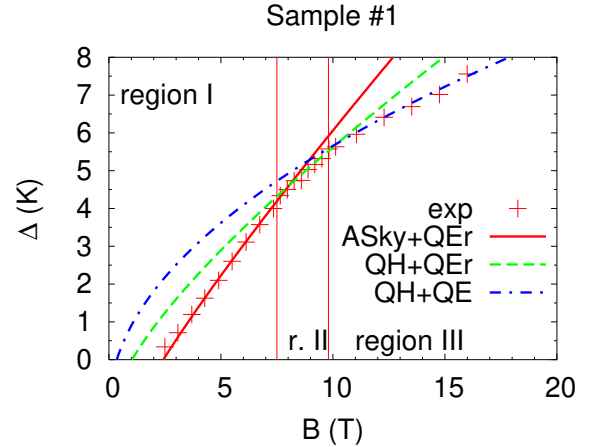


FIG. 9: Gap energies of the sample # 1 (Fig. 2) interpreted as an antiskyrmion plus QEr for low B (region I) and a QE{QH} pair for high B (region III). The disorder-induced gap reduction (E_d) obtained by fitting is 3.2 K, 1.8 K and 1.4 K for region I, II and III, respectively.

Let us first focus on the low field region I, Fig. 9. The experimental data show a remarkably precise linear behaviour. Within the uncertainty of the measurement, this linearity does not necessarily mean that the Coulomb contribution to the gap entirely vanishes, but it sets a rather stringent upper limit of approximately $E_C < 0.025$. We are then left merely with two possibilities: either $(S_z \sim) = 3$ and E_C is zero or $(S_z \sim) = 2$

and $E_C = 0.02$. The exact diagonalization spectra indicate that for $B < 4.5$ T a $K_A = 1$ antiskyrmion is energetically more favourable than a bare quasi-hole or a ASky(2), Fig. 4. On the other hand, even the smallest skyrmion $K_S = 1$ costs more energy in this range of magnetic fields than a quasielectron with reversed spin. Therefore, in this case, the most likely pair of charged particles created by a thermal excitation will be a QEr{ASky ($K_A = 1$). Energetical cost of this excitation, two spins plus Coulomb energy $E_C = 0.035 - 0.011 = 0.024$, Subsect. IIIC, is in a nice agreement with the experimental data, Fig. 9.

As the magnetic field increases, the $K_A = 1$ antiskyrmion becomes more energetically costly than a plain quasi-hole. The gap should then amount to creation of a QH{QEr pair, i.e. to one spin up plus $E_C = 0.035$. It is not guaranteed that we indeed observe this excitation in the measurement: region II is not very large, Fig. 9, and it could well be, that what we observe here is just a smooth transition between regions I and III. Despite this, we should like to point out, that the exact diagonalization energies are compatible with the QH{QEr interpretation of region II.

Finally, for yet higher magnetic fields, it is more favourable to create a quasielectron in a higher CF LL than to flip its spin. In line with the situation of the $B \rightarrow 1$ limit, we expect a QH{QE pair without reversed spin to be the lowest excitation, Fig. 4. Indeed, the best fit in region III has $E_C = 0.045 - 0.005$ and zero Zeeman energy. This Coulomb energy is however almost by a factor of 2 smaller than $E_{CDW}(k \neq 1)$ from the exact diagonalization, Fig. 6 and table II. Therefore, let us focus on region III now.

The only alternative interpretation of region III is that we observe a QH{QEr pair here (while region II is just the smooth transition between the two other adjacent regions). This scenario is not very likely though. With one spin up included, Eq. (6) implies that the Coulomb energy in region III could not exceed 0.010. There is no justification for such an excitation within the ED spectra in the $S = N = 2 - 1$ sector, Fig. 5. Also, with this scenario, the gap reduction constant would be negative (around -1 K).

With the interpretation of $E_C = 0.045$, $S_z = 0$ it is remarkable how near this value lies to the energy of the magnetoroton minimum, Fig. 6 (Table II). It is tempting to conclude that the activation process goes in two steps, creation of a magnetoroton and unbinding of the constituent QE and QH. The former step costs more energy, roughly $E_{CDW}(1.4 \cdot 10^{-1}) = 0.05$ in Coulomb units as compared to $E_{CDW}(k \neq 1) = E_{CDW}(1.4 \cdot 10^{-1}) = 0.08 - 0.05 = 0.03$ for the unbinding of a magnetoroton. The creation is therefore a bottleneck for the whole activation process and it determines the activation energy measured in transport in the limit of high Zeeman energies. Such a two-step process is not possible for the spin-flip excitations because the spin wave dispersion has no minimum which could lead to a stable intermediate

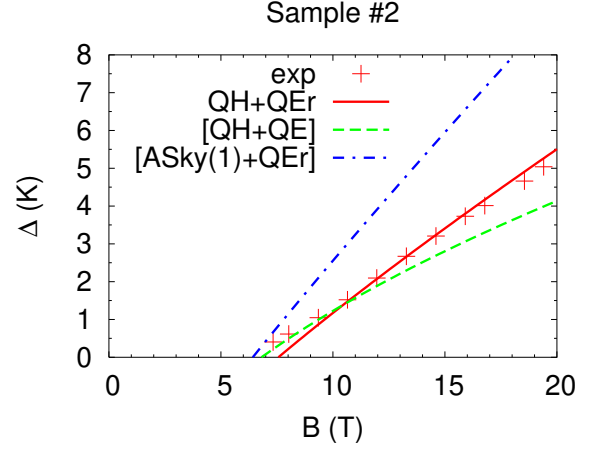


FIG. 10: Gap energies of the sample # 2 (Fig. 2) interpreted as a spinwave (a QH{QEr pair). The gap reduction 5.8 K is larger than for the sample # 1. For other options (2 spins = ASky(1)+QEr and 0 spins = QE+QH), the parameters were taken as in Fig. 9, only the constant offset E_d was adjusted.

state. We wish to stress that the activation gap smaller than the theoretical predictions of $E_{CDW}(k \neq 1)$ has been observed many times^{42,43,44} but the problem was never conclusively resolved. Usually, this discrepancy was as a whole attributed to the disorder. Here we propose that the smaller observed gap for no-spin excitations is only in part due to the disorder. For the sample # 1, this B-independent reduction is $E_d = 1.4$ K. The other, ‘traditional’, interpretation that the disorder reduces the Coulomb energy, meaning $E_d = 0$ and a modified value of E_C in (6), is in conflict with the gaps observed in region I, Fig. 9. It should be noted that we indeed found different gap reductions for different excitations within the same sample, Fig. 9. An attempt to use the value of E_d related to ASky(1)+QEr (region I) also for region III leads to only a slightly changed E_C while the quality of the fit is apparently worse.

The data of sample # 2 suggest that we measure a QH{QEr pair in the whole range of accessible magnetic fields, Fig. 10. The ED energy of a spin wave is somewhat larger than what the experimental data suggest (0.025). Other explanations, however, are unlikely. Excitations with two spins (e.g. skyrmions) lie well above the measured gaps, even if we assume zero Coulomb energy of such an excitation. Spinless excitations, on the other hand, lead to $\Delta(B)$ which is too far away from a linear dependence seen in Fig. 10. As an example we took the two-spin (ASky+QEr) and zero-spin (QH+QE) excitations as discussed for sample # 1, adjusted E_d and plotted them into Fig. 10 as a dash-dotted and dashed line, respectively.

The absence of skyrmionic excitations for sample # 2 is not surprising given its lower mobility. Lower quality means larger disorder-induced gap reduction ($E_d = 6$ K)

implying a higher FQHE threshold in B ($B \approx 7$ T), cf. Fig. 10 and 9. These are too high fields for (anti)skyrmions to be observed, Fig. 4. Less obvious is the absence of a transition to a spinless excitation (QE+QH) as the one observed for sample #1. We find, however, that such an excitation would be observable below 20 T only if E_d for QE+QH were > 5 K. By comparison with typical gap reductions in sample #1 this seems unlikely.

The present measurements suggest that, paradoxically, single spin- \uparrow excitations may be observed up to rather high magnetic fields (20 T) even in samples with mobility below $100 \text{ m}^2/\text{Vs}$. However, in order to observe larger (anti)skyrmions in FQH systems the Zeeman energy should be suppressed⁴⁵. By applying the hydrostatic pressure and reducing the Lande g -factor, the maximum of three spin- \uparrow s per excitation was reached⁵ compared to two spin- \uparrow s of our experiment. In an ideal case, one should be able to observe more transitions in (B) , not just one as in Fig. 9, corresponding to successive reduction of skyrmion and antiskyrmion sizes with increasing magnetic field (or Zeeman energy) at fixed filling factor.

V. CONCLUSION

Spin excitations in the $\nu = \frac{1}{3}$ FQH system were studied using measurements of the activation gap, Δ , as a function of magnetic field. Supported by energies obtained by exact diagonalization we identified the activation-relevant excitation to be a spin wave in the sample #2 and an antiskyrmion with one spin- \uparrow plus a quasielectron with reversed spin for the sample #1. The abrupt change in (B) observed at $B \approx 9$ T in the sample #1 was attributed to the transition to a charge density wave in the lowest excitation. Since the gap was in this case

smaller than what we would expect for a charge density wave with finite wavevector, we proposed that the activation is a two-step process with magnetoroton minimum governing the activation energy as a bottleneck. With this interpretation, we found the effect of disorder to be a constant reduction E_d of the gap, independent on magnetic field, in agreement with previous works^{21,22}. Consistent with its lower mobility, the gap reduction is larger for sample #2 and it is different for different types of excitations.

In order to obtain a quantitative agreement between the energies from the exact diagonalization and the experiment, finite thickness as well as the Landau level mixing up to the first order have to be included. We wish to stress that the number of spin- \uparrow s involved in the particular excitations can be determined with very high certainty even with little knowledge of the Coulomb energy. This is on one hand owing to the precision of the experimental data showing linear (B) and on the other hand because the number of spin- \uparrow s should be an integer. Our only fitting parameter was the constant disorder-induced reduction of the activation gap.

Acknowledgements

It is our pleasure to thank Eros Mariani and Daniela Pfannkuche for worthwhile discussions. AD and RH acknowledge support via DFG priority program "Quanten Hall Systeme" and BM BF, AW acknowledges support from the grant 2P03B02424 of the Polish MENiS and KV and OC acknowledge the support by the Academy of Sciences of the Czech Republic and its Grant Agency under Institutional Support No. AV0Z10100521 and by the Ministry of Education of the Czech Republic Center for Fundamental Research LC510.

- ¹ S. Barrett, G. Dabbagh, L. Pfeiffer, K. West, and R. Tycko, *Phys. Rev. Lett.* **74**, 5112 (1995).
- ² A. Schmeier, J. Eisenstein, L. Pfeiffer, and K. West, *Phys. Rev. Lett.* **75**, 4290 (1995).
- ³ E. Aifer, B. Goldberg, and D. Broido, *Phys. Rev. Lett.* **76**, 680 (1996).
- ⁴ D. Maude, M. Potemski, J. Portal, M. Henini, L. Eaves, G. Hill, and M. Pate, *Phys. Rev. Lett.* **77**, 4604 (1996).
- ⁵ D. R. Leadley, R. J. Nicholas, D. K. Maude, A. N. Ustizh, J. C. Portal, J. J. Harris, and C. T. Foxon, *Phys. Rev. Lett.* **79**, 4246 (1997).
- ⁶ O. Heinonen, ed., *Composite fermions* (World Scientific, 1998).
- ⁷ H. Fertig, L. Brey, R. Côté, and A. MacDonald, *Phys. Rev. B* **50**, 11018 (1994).
- ⁸ S. Sondhi, A. Karlhede, S. Kivelson, and E. Rezayi, *Phys. Rev. B* **47** (24), 16419 (1993).
- ⁹ D. Lee and C. Kane, *Phys. Rev. Lett.* **64**, 1313 (1990).
- ¹⁰ K. Moon, H. Mori, K. Yang, S. G. Irvin, A. MacDonald, L. Zheng, D. Yoshioka, and S.-C. Zhang, *Phys. Rev. B*

- 51**, 5138 (1995).
- ¹¹ X. Xie and S. He, *Phys. Rev. B* **53**, 1046 (1996).
- ¹² A. Wojs and J. Quinn, *Phys. Rev. B* **66**, 045323 (2002).
- ¹³ E. Rezayi, *Phys. Rev. B* **43**, 5944 (1991).
- ¹⁴ E. Rezayi, *Phys. Rev. B* **56**, 7104R (1997).
- ¹⁵ X.-G. Wu and S. Sondhi, *Phys. Rev. B* **51**, 14725 (1995).
- ¹⁶ E. Rezayi, *Phys. Rev. B* **36**, 5454 (1987).
- ¹⁷ R. Kamilla, X. Wu, and J. Jain, *Surf. Sci.* **99**, 289 (1996).
- ¹⁸ A. MacDonald and J. Palacios, *Phys. Rev. B* **58** (16), R10171 (1998).
- ¹⁹ T. Chakraborty and P. Pietiläinen, *Phys. Rev. Lett.* **76** (21), 4018 (1996).
- ²⁰ P. Khandelwal, N. Kuzma, S. Barrett, L. Pfeiffer, and K. West, *Phys. Rev. Lett.* **81**, 673 (1998).
- ²¹ R. Morf and N. d'Ambrumenil, *Phys. Rev. B* **68**, 113309 (2003).
- ²² A. F. Dethlefsen, E. Mariani, H.-P. Tranitz, W. Wegscheider, and R. J. Haug, *cond-mat/0508393* (2005).
- ²³ A. Wojs and J. Quinn, *Phys. Rev. B* **61**, 2846 (2000).
- ²⁴ S.-Y. Lee, V. Scarola, and J. Jain, *Phys. Rev. B* **66**,

- 085336 (2002).
- ²⁵ T. Chakraborty and P. Pietiläinen, *The Quantum Hall Effects* (Springer, Berlin, 1995), 2nd ed.
 - ²⁶ D. Yoshioka, *The Quantum Hall Effect* (Springer, Berlin, 2002).
 - ²⁷ F. Haldane, *Phys. Rev. Lett.* **51**, 605 (1983).
 - ²⁸ D. Yoshioka, B. Halperin, and P. Lee, *Phys. Rev. Lett.* **50**, 1219 (1983).
 - ²⁹ D. Yoshioka, *Phys. Rev. B* **29**, 6833 (1984).
 - ³⁰ F. Haldane and E. Rezayi, *Phys. Rev. B* **31**, 2529R (1985).
 - ³¹ C. Nayak and F. Wilczek, *cond-mat/9507016* (1995).
 - ³² T. Chakraborty **229**, 16 (1990).
 - ³³ T. Chakraborty and P. Pietiläinen, *Phys. Rev. B* **41**, 10862 (1990).
 - ³⁴ R. Laughlin, *Phys. Rev. Lett.* **50**, 1395 (1983).
 - ³⁵ T. Chakraborty, P. Pietiläinen, and R. Shankar, *Europhys. Lett.* **38** (2), 141 (1997), (*cond-mat/9703108*).
 - ³⁶ A. MacDonald and G. Aers, *Phys. Rev. B* **29**, 5976 (1984).
 - ³⁷ F. Zhang and S. DasSarma, *Phys. Rev. B* **33**, 2903 (1986).
 - ³⁸ T. Ando, A. Fowler, and F. Stem, *Rev. Mod. Phys.* **54**, 437 (1982).
 - ³⁹ R. Morf, N. d'Ambrosio, and S. DasSarma, *Phys. Rev. B* **66**, 075408 (2002).
 - ⁴⁰ D. Yoshioka, *J. Phys. Soc. Jpn.* **55**, 885 (1986).
 - ⁴¹ K. Vybomy, Ph.D. thesis, Universität Hamburg (2005), www.sub.uni-hamburg.de/opus/volltexte/2005/2553.
 - ⁴² R. Willett, H. Stormer, D. Tsui, A. Gossard, and J. English, *Phys. Rev. B* **37**, 8476 (1988).
 - ⁴³ G. Böbinger, A. Chang, H. Stormer, and D. Tsui, *Phys. Rev. Lett.* **55**, 1606 (1985).
 - ⁴⁴ G. Böbinger, H. Stormer, D. Tsui, A. Chang, J. Hwang, A. Cho, C. Tu, and G. Weinmann, *Phys. Rev. B* **36**, 7919 (1987).
 - ⁴⁵ I. Kukushkin, K. von Klitzing, and K. Eberl, *Phys. Rev. B* **60**, 2554 (1999).